



Impact of dissolved organic carbon on per- and polyfluoroalkyl mobility in activated carbon-amended soils[☆]

Georgios Niarchos^{a,b,*}, Lutz Ahrens^b, Dan B. Kleja^c, Anna Merle Liebenehm Axmann^a, Fritjof Fagerlund^a

^a Department of Earth Sciences, Uppsala University, P.O. Box 256, SE-751 05, Uppsala, Sweden

^b Department of Aquatic Sciences and Assessment, Swedish University of Agricultural Sciences (SLU), P.O. Box 7050., SE-750 07, Uppsala, Sweden

^c Department of Soil and Environment, Swedish University of Agricultural Sciences (SLU), P. O. Box 7090., SE-750 07, Uppsala, Sweden

ARTICLE INFO

Keywords:

Colloidal activated carbon
Dissolved organic carbon
Transport
Adsorption
Desorption
Remediation

ABSTRACT

The remediation of per- and polyfluoroalkyl substances (PFASs) remains a formidable challenge due to their recalcitrance and complex environmental behaviour. Dissolved organic carbon (DOC) plays a critical, yet insufficiently understood role, in modulating PFAS fate, transport, and the efficacy of remediation strategies. This study employs dynamic column experiments under environmentally relevant conditions to elucidate the influence of DOC on the sorption and mobility of fourteen PFASs in reference soils and soils treated with colloidal activated carbon (CAC). Results demonstrate that DOC significantly reduces PFAS sorption in CAC-treated soils, leading to increased aqueous phase concentrations of PFAS. The presence of DOC decreased soil-water partitioning coefficients (K_d values) for all PFASs by an order of magnitude, with long-chain PFASs and fluorotelomersulfonic acids (FTSAs) exhibiting the most pronounced decreases, by as much as 40-fold. Mass balance data showed that DOC increased PFAS elution by up to 10-fold in CAC-treated soils. The PFAS breakthrough curves revealed enhanced PFAS mobility in the presence of DOC, particularly in carbon-amended soils. These results underscore the critical role of DOC in facilitating PFAS transport, with significant implications for their persistence, risk assessment, and the optimization of sorbent-based remediation strategies in organic-rich environments.

1. Introduction

Per- and polyfluoroalkyl substances (PFASs) are a broad category of synthetic compounds that have left an indelible mark on our ecosystems. They encompass thousands of distinct congeners, with approximately 15,000 unique chemical structures according to the USEPA's CompTox database (USEPA, 2022). PFASs exhibit hydro- and oleophobicity, low surface tension, and chemical inertness, owing to the strength of carbon-fluorine (C-F) bonds (Buck et al., 2011). These distinctive attributes make them valuable in various applications but also enable their persistence and bioaccumulation, putting humans and other living organisms in danger (Dickman and Aga, 2022).

PFAS regulatory measures have been tightening since the early 2000s, after the inclusion of perfluorooctane sulfonic acid (PFOS), its

salts, and perfluorooctane sulfonyl fluoride (PFOSF) in the list of persistent organic pollutants (POPs) (United Nations Environment Programme (UNEP), 2009). With increasing restriction of legacy PFASs, their production and use have shifted to alternative PFASs, often including short-chain compounds (Wang et al., 2019). These substitutes, however, are characterised by increased mobility, while the assumption of their low toxicity is not only debated but increasingly unlikely (Ateia et al., 2019; Li et al., 2020; Woodlief et al., 2021). In the absence of viable replacements and lack of holistic restrictions, preventing their further spread remains a priority.

Effectively mitigating the omnipresence of PFASs, requires targeted treatment of contaminated hotspots. Activated carbon has emerged as a leading solution for soil stabilization due to its strong PFAS adsorption capacity (Ross et al., 2018; Söregård et al., 2021, 2019). A key

[☆] This paper has been recommended for acceptance by Dr Jiayin Dai.

* Corresponding author. Department of Aquatic Sciences and Assessment, Swedish University of Agricultural Sciences (SLU), P.O. Box 7050., SE-750 07, Uppsala, Sweden.

E-mail addresses: georgios.niarchos@slu.se (G. Niarchos), lutz.ahrens@slu.se (L. Ahrens), dan.berggren@slu.se (D.B. Kleja), fritjof.fagerlund@geo.uu.se (F. Fagerlund).

<https://doi.org/10.1016/j.envpol.2025.126928>

Received 9 April 2025; Received in revised form 1 July 2025; Accepted 30 July 2025

Available online 5 August 2025

0269-7491/© 2025 The Authors. Published by Elsevier Ltd. This is an open access article under the CC BY license (<http://creativecommons.org/licenses/by/4.0/>).

advancement is the use of colloidal activated carbon (CAC), a liquid activated carbon™ that can be injected into the subsurface and form a permeable reactive barrier (PRB) within the groundwater zone, limiting PFAS leaching and migration (Carey et al., 2022; Niarchos et al., 2022; Sorengard et al., 2019).

The effectiveness of activated carbon treatment in PFAS soil treatment is governed by PFAS properties, such as carbon chain length and surface charge, and not least by environmental factors (Du et al., 2014). Organic matter, which is naturally abundant in soils, exists in different forms that can have contrasting effects on contaminant mobility; particulate organic carbon can retard the movement of pollutants through sorption or physical blocking, while dissolved organic carbon (DOC) can enhance pollutant transport by increasing solubility or facilitating co-transport (Iubel et al., 2021; McDowell, 2003). DOC is the dissolved fraction of organic matter ($\phi < 0.45 \mu\text{m}$) and consists of highly soluble aliphatic and aromatic hydrocarbons, such as fulvic acid (Lønborg et al., 2024; Piccolo, 2002; Totsche et al., 1997). DOC concentrations vary across space and time, with levels in groundwater systems typically ranging between 0.5 mg L^{-1} to 30 mg L^{-1} (McDonough et al., 2020; Vidon and Hill, 2004; Werner et al., 2021). Higher DOC levels are often associated with slower sorption kinetics. For some organic contaminants, such as polycyclic aromatic hydrocarbons (PAHs), there has been evidence of DOC enhancing retention in clay particles (Totsche et al., 1997). However, the effects of DOC on PFAS sorption are more complex and can vary based on the environmental context and the properties of the sorbent (Kabiri et al., 2024). In groundwater, DOC has been observed to both hinder and enhance PFAS sorption; Qi et al. (2022) reported that organic matter can increase PFAS sorption in sediments, but it may also compete with PFAS for binding sites in artificial sorbents, limiting treatment efficiency. Wen et al. (2016) demonstrated that the bioconcentration of perfluoroalkyl acids (PFAAs) depends significantly on the composition of DOM rather than its overall concentration (Liu et al., 2019; Qi et al., 2022). Ulrich et al. (2015) showed that higher DOC levels can result in lower soil-water partitioning coefficients (K_d values) and slower sorption kinetics for trace organic contaminant retention in biochar. Jeon et al. (2011) have also found an increase of PFAS concentrations in the aqueous phase, when DOM was released from coated clay particles.

Despite growing research, the role of DOC in PFAS transport through soils and its impact on soil treatment remain insufficiently understood. This study aims to fill this critical gap by determining the impact of DOC on PFAS mobility in soils and groundwater. Column experiments were conducted, to simulate contaminant transport under dynamic conditions (Van Glubt et al., 2021). The primary objectives of the study were to: i) assess the influence of DOC on PFAS sorption-desorption behaviour in soil with and without activated carbon amendments, ii) quantify the extent to which DOC alters PFAS transport, and iii) evaluate the environmental implications of DOC-driven PFAS mobility, particularly the challenges it presents for effective remediation.

2. Materials and methods

2.1. Soil sampling and preparation

Soil was sampled at a reference point, close to a contaminated site ($59^{\circ}23'13.7''\text{N}$, $15^{\circ}53'48.2''\text{E}$) in Sweden, at a depth of 3 m (Niarchos et al., 2023a). Subsequently, the soil was air dried at 40°C in a dust-protected room, ground and sieved to eliminate large particles ($>2 \text{ mm}$) and homogenised through shaking. Based on texture analysis, the soil was characterised as a silt loam, while it exhibited very low levels of organic carbon, which is typical for deeper subsoils and groundwater zones, and PFAS (Tables S1 and S2 in SI). Before being packed into the columns, the soil was mixed with premium #40/50 silica sand (AGSCO, USA) at a 1:5 ratio (field soil:silica sand) to enhance the hydraulic conductivity of the columns and better simulate aquifer conditions. The samples were also analysed for PFAS content, based on the procedure

described in Section 2.4 (Table S3 in Supporting Information (SI)).

For the treated soil columns, soil was mixed with CAC (PlumeStop®, Regenesis) at a final activated carbon concentration of 0.1 \% w/w (dry), which corresponds to concentrations applied in the field (Niarchos et al., 2023a). The treatment process involved spiking the sampled soil with fresh PlumeStop®, followed by mixing it with the appropriate sand amount in end-over-end shakers over a 24-hr period.

2.2. Experimental setup and column specifications

Miscible displacement experiments were conducted, by simulating typical aquifer conditions in column experiments (i.e., with water-saturated and convection-dominated flow regimes). The experimental setup closely follows the methodology detailed in our prior study (Niarchos et al., 2022), with minor adjustments made for this study, described briefly in the following. Transparent polyvinyl chloride (PVC) columns measuring 15 cm in length and 3.6 cm in diameter were employed to emulate field conditions. A total of eight column experiments were conducted, including duplicate tests for CAC-treated soil exposed to artificial groundwater without DOC (T1, T2), CAC-treated soil exposed to artificial groundwater containing DOC ($T_{\text{DOC}1}$, $T_{\text{DOC}2}$), reference soil (same substrate but without CAC) exposed to artificial groundwater without DOC (R1, R2), and reference soil exposed to artificial groundwater containing DOC ($R_{\text{DOC}1}$, $R_{\text{DOC}2}$) (see Table 1 for details).

Soil was packed into the columns ensuring a homogeneous matrix, by gradually adding dry soil in small portions while saturating it with inflow water from the bottom and vibrating it to eliminate entrapped air. The total weight of dry soil was $281 \pm 6 \text{ g}$. Pre-equilibration of the columns was carried out by pumping artificial groundwater through them for 48 h , using a multichannel peristaltic pump (ISM931C, Simatic® IPC, Germany) at a flow rate of 200 mL d^{-1} . The pre-equilibration step did not include the introduction of DOC to the columns; this allowed for concurrent interactions between DOC and PFAS in the bulk material.

In four columns, the impact of DOC was evaluated by spiking the inlet water with 20 mg L^{-1} nominal Suwannee River Fulvic Acid (SRFA). Given that SRFA consists of approximately 50 \% carbon by mass, this corresponds to a DOC concentration of approximately 10 mg L^{-1} , which is at the high end of global groundwater concentrations, according to McDonough et al. (2020). Water spiked with DOC was stored in the dark, in white HDPE bottles, to prevent degradation of organic matter and decrease potential microbial activity. Positive controls were obtained directly at the entrance of the columns using a three-way valve on two occasions, one at the beginning and one at the end of the spiking, and the average was used as representative of the inflow concentration (C_0) for

Table 1

Overview of the column experiments and their operational conditions. C_{CAC} refers to the starting concentration of CAC in the treated soil, C_{DOC} is the concentration of DOC as fulvic acid in the inlet water, and $C_{\Sigma 14\text{PFAS}}$ is the starting concentration of the sum of PFAS in the inlet water.

Column ID	Matrix	C_{CAC} (w/w)	C_{DOC} (mg L^{-1})	$C_{\Sigma 14\text{PFAS}}$ (mg L^{-1}) ^a	Flow rate (mL d^{-1})	pH
R1	Reference	–	–	1.0	200	7.3
R2	soil					
T1	CAC-treated	0.1 %				
T2	soil					
$R_{\text{DOC}1}$	Reference	–	10			
$R_{\text{DOC}2}$	soil					
$T_{\text{DOC}1}$	CAC-treated	0.1 %				
$T_{\text{DOC}2}$	soil					

^a PFAS-spiked artificial groundwater (1 mg L^{-1} for 14 individual PFAS in equimass concentrations) for the first 223 pore volumes (PV), followed by PFAS-free artificial groundwater to assess their leaching potential (desorption phase) until 291 PV.

each column.

A total of 291 pore volumes (PV) were flushed through the columns at a constant flow rate of 200 mL d⁻¹. The first 223 PV consisting of PFAS-spiked artificial groundwater (1 mg L⁻¹ for the sum of 14 individual PFAS in equimass concentrations), followed by PFAS-free artificial groundwater to assess their leaching potential during the desorption phase until 291 PV. The total number of samples were $n = 20$ per column. The applied PFAS concentration represents a high-end, worst-case scenario typical of severely impacted sites such as firefighting training areas, and was selected to allow for better observation of sorption dynamics and potential saturation effects under stress conditions (Johnson et al., 2022).

2.3. Chemicals and materials

The feed solution was spiked with a mixture of 14 PFAS in methanol, including C₃-C₁₀ perfluorocarboxylic acids (PFCAs): perfluorobutanoic acid (PFBA), perfluoropentanoic acid (PFPeA), PFHxA, perfluoroheptanoic acid (PFHpA), PFOA, perfluorononanoic acid (PFNA), PFDA, perfluoroundecanoic acid (PFUnDA); C₄, C₆, C₈ perfluoroalkyl sulfonates: perfluorobutane sulfonic acid (PFBS), perfluorohexane sulfonic acid (PFHxS), PFOS; perfluorooctane sulfonamide (FOSA); and 6:2 and 8:2 fluorotelomersulfonic acids (FTSA). The methanol content in the final solution was <0.1 %, to avoid co-solvent effects (Schwarzenbach et al., 2002). The DOC was introduced to the inlet solution of four columns by adding SRFA, purchased by the International Humic Substances Society (IHSS).

The following isotopically labelled internal standards were employed for quantifying the target PFAS: perfluoro-(¹⁸O₂)-hexane sulfonic acid (¹⁸O₂-PFHxS), perfluoro-(¹³C₄)-octane sulfonic acid (¹³C₄-PFOS), perfluoro-(¹³C₂)-hexanoic acid (¹³C₂-PFHxA), perfluoro-(¹³C₅)-nonanoic acid (¹³C₅-PFNA). Both native and mass-labelled standards were purchased from Wellington Laboratories and had a purity >98 %. Other chemicals, including HPLC-grade methanol (purity >99.9 %) and calcium chloride anhydrous (CaCl₂, purity >99.99 %), were obtained from Sigma Aldrich. CAC (PlumeStop®) was provided by Regenesis. Further information on the CAC material is available in Table S4 in SI.

2.4. PFAS analysis

Samples were collected from the inlet and outlet of the columns at specified intervals for chemical analysis of the targeted PFASs. The analysis was performed using ultra high-performance liquid chromatography coupled with tandem mass spectrometry (UHPLC-MS/MS, Quantiva TSQ; Thermo Fischer Scientific, USA). Water samples were analysed via direct injection following a cleanup step with ENVI-carb and centrifugation, while soil samples underwent solid-liquid extraction, following established methods (Ahrens et al., 2009). Briefly, after addition of an internal standard (IS) mixture, methanol was used for solid-liquid extraction followed by centrifugation (3000 rpm, 15 min) and filtration through a 0.45 µm recycled cellulose (RC)-syringe filter, resulting in 1:1 methanol:water aliquots. Blanks ($n = 2$) and positive controls ($n = 2$) were also included in the analysis, following the same procedure. Method detection limits ranged from 0.05 to 0.5 ng mL⁻¹ (Table S5 in SI), and the average recovery of IS was 110 ± 4 % (for details, see Table S6 in SI). For the statistical analysis, the significance threshold was set at 0.01.

2.5. Tracer tests

Tracer tests were performed to estimate column parameters and compare the retardation factors of the tracer to those of PFASs. Sodium chloride (NaCl) was used as a conservative tracer at a concentration of 0.43 M. The experimental procedure began with a four-day calibration period for the columns, to ensure steady-state conditions. Following calibration, the tracer solution was injected into the column, over

approximately 24 h. The pulse duration was between 23 and 31 h. The evolution of the tracer was continuously monitored using in-line conductivity meters connected to the outlet, logging the temperature-adjusted conductivity every 10 s. After the tracer injection, the inflow was switched from the tracer solution to artificial groundwater to allow the column to re-equilibrate over a period of three days. Subsequently, the appropriate feed solution, as specified in Table 1, was introduced into the column.

2.6. Determination of organic carbon on soil materials

Organic carbon analysis was used to estimate carbon retention in the columns after the experiments. Soil carbon and nitrogen content were determined using International Organisation for Standardisation (ISO) 10694 (1995) and ISO13878 (1998) standards, employing a TruMac® CN elemental analyser. In brief, samples underwent combustion in pure O₂ at 1350 °C, converting carbon and nitrogen to CO₂ and NO_x. The CO₂ mass, converted to percent carbon, was measured based on the dry sample weight. A portion of the gas, transported by pure He, underwent reduction by Cu in a designated zone, converting NO_x to N₂ and measured by a thermal conductivity detector. Total carbon (TC) and total inorganic carbon (TIC) contents of each sample were determined in two separate runs allowing for the calculation of the total organic carbon content, as %TOC = %TC - %TIC. The results of the analysis can be seen in Table S7 in SI.

3. Results and discussion

3.1. Tracer tests

The breakthrough curves (BTCs) of the conservative tracer tests, shown in Fig. S1 in the SI, offer insights into the transport dynamics within the reference and CAC-treated soils. The overall similarity in BTC shapes suggests consistent column packing and steady-state conditions across all experiments. However, the slight asymmetries observed in some BTCs, such as delayed peaks or extended tails, indicate subtle differences in flow patterns or interactions with soil or CAC.

Most columns had a noticeable tailing effect following the tracer peak, suggesting some degree of dispersion and potential interactions between the tracer and the soil matrix, that can influence the tracer's transport. The tailing effect was more pronounced for columns R1, R_{DOC1}, and R_{DOC2}, as they exhibited a higher slope at the latter part of the graph. The decreased tailing in the CAC-treated soil columns could also be indicative of CAC mitigating dispersion.

Columns with DOC also showed a slightly different behaviour to the ones without DOC. Specifically, in both treated and reference soil columns, the BTCs exhibited more pronounced tailing with DOC, indicating increased interaction between the tracer and the DOC. Additionally, salts can reportedly form complexes with organic matter in the soil and induce flocculation (Khoo et al., 2022), which could influence their transport behaviour.

The average pore water velocity was estimated using the formula the formula $\bar{v} = \frac{L}{t_{0.5}}$, where $t_{0.5}$ is the time required for the tracer to reach C/C₀ = 50 % in the outlet, and L is the length of the column equal to 15 cm. For all experiments, the average pore water velocity was $\bar{v} = 2.14 \pm 0.29$ cm h⁻¹ ($n = 8$), which is representative of silty sand aquifer conditions (Fetter, 2018). Comparing the reference and treated soils, the BTCs had a slightly faster and more uniform tracer transport for the treated soils compared to the reference soils. Specifically, faster breakthrough and higher pore water velocities were observed in the reference soil (for R1, R2, R_{DOC1}, R_{DOC2}, $\bar{v} = 2.33$ cm h⁻¹) compared to the treated soil columns (for T1, T2, T_{DOC1}, T_{DOC2}, $\bar{v} = 1.96$ cm h⁻¹). This suggests that the soil treatment with CAC has slightly altered the soil structure, possibly reducing the effective pore size, or by making the pore spaces more tortuous.

3.2. PFAS breakthrough

3.2.1. Reference soil

The BTCs for the targeted PFASs in reference soil with and without DOC are shown in Fig. 1. Many compounds exhibited complete breakthrough rapidly, particularly short-chain PFASs. However, differences in breakthrough behaviour could be noticed for longer chain PFASs and when DOC was present.

The presence of DOC resulted in broader BTC peaks and increased tailing for several PFASs, including PFUnDA and PFOS, indicating enhanced mobility. Additionally, for FOSA, PFOS, and 8:2 FTSA, the initial phase of the breakthrough curve exhibited a delay in concentration increase in the presence of DOC, suggesting enhanced sorption of these PFASs under these conditions.

Effluent concentrations exceeding influent levels ($C/C_0 > 1$) were observed for several PFASs, including PFHxA, PFHpA, PFOS, and PFUnDA, which is indicative of competitive sorption dynamics. This overshoot effect can be attributed to chromatographic displacement, where more hydrophobic compounds displace previously sorbed PFASs, leading to remobilization (McCleaf et al., 2017; Niarchos et al., 2022; Park et al., 2020). This effect can be induced by competition among PFASs (Niarchos et al., 2023b), however, in the present study overshoot concentrations were mainly associated with DOC (Fig. 1).

DOC amplified desorption and prolonged the release of PFASs during the desorption phase ($PV > 223$). In the absence of DOC, PFAS concentrations declined upon transitioning to PFAS-free water. Conversely, in the presence of DOC, concentrations continued to increase well after the switch to PFAS-free water, in some cases exceeding the initial influent concentration (e.g., for 6:2 FTSA, 8:2 FTSA, PFOA, PFUnDA, $C/C_0 \gg 1$). These findings demonstrate that DOC accelerates desorption kinetics, but also reduces long-term retention, likely through competitive displacement at sorption sites or direct PFAS complexation with DOC in solution (Iubel et al., 2021). Furthermore, DOC can increase the negative surface charge of soil particles (Klučáková, 2018), which may exacerbate electrostatic repulsion of anionic PFASs, thereby reducing long-term retention resulting in less PFAS being trapped in the soil.

3.2.2. CAC-treated soil

The BTCs in the CAC-treated soil columns (Fig. 2) reveal a more pronounced influence of DOC on PFAS sorption compared to the reference soil columns (Fig. 1). In all instances, DOC led to higher PFAS groundwater concentrations, indicating a reduction in sorption effectiveness. Complete breakthrough ($C/C_0 = 1$) was not reached for any of the targeted PFASs during the experiments, indicating strong sorption to CAC. Short-chain PFASs exhibited faster breakthrough, as was expected due to their lower affinity to carbon and higher solubility (Hansen et al., 2010). The presence of DOC consistently led to higher relative concentrations for almost all targeted PFASs, demonstrating a general trend of decreased sorption efficiency in DOC-rich conditions.

Furthermore, a sustained increase in PFAS concentrations during the desorption phase was evident for most PFASs, with the exceptions of PFBA, PFHxA, and PFHpA. This trend, albeit to a lesser extent, was also evident in the reference soil columns (Fig. 1). As DOC continued to be introduced during the desorption phase, it might have outcompeted certain PFASs, thereby reducing PFAS partitioning onto CAC particles. The area under the curve (AUC) of each BTC represents the total eluted PFAS mass, with a larger area (indicating greater mass elution) observed under the influence of DOC. This suggests that DOC reduces PFAS retention in soil, with a more pronounced effect in CAC-treated soil, implying a significant role of DOC in diminishing PFAS sorption. One possible mechanism is the formation of PFAS-DOC complexes in solution, which could enhance PFAS mobility (Iubel et al., 2021). Schwichtenberg et al. (2020), also reported that naturally occurring DOC significantly contributes to PFAS foam formation, indicating strong interactions between DOC and PFASs in both aqueous and sorbed phases. DOC can also increase the formation of biofilm in subsurface

environments, which may in turn influence PFAS sorption and desorption (Penland et al., 2020; Voisin et al., 2020).

3.3. Partitioning coefficients

Partitioning coefficients were estimated by assuming linear sorption. The retardation factors for each column were calculated using the formula $R_f = \frac{t_{50, NaCl}}{t_{50, PFAS}}$, where t_{50} represents the time required to reach 50 % breakthrough for the conservative tracer (NaCl) and each PFAS compound. Linear regression was used to estimate the center of mass of the BTCs, at 50 % PFAS breakthrough for PFASs ($t_{50, PFAS}$) and the tracer ($t_{50, NaCl}$) (for reference, see Fig. S1 in the SI, Figs. 1 and 2). Partitioning coefficients (K_d , L kg⁻¹) were calculated in accordance with USEPA (1999) guidelines, as $K_d = (R_f - 1) \cdot n_{eff} / \rho$, where n_{eff} represents the effective porosity, and ρ the bulk density of the packed soil. The effective porosity, n_{eff} , was computed as 0.30 % of the total column volume. The bulk density, ρ , of the soil mixture was determined to be 2.01 g cm⁻³, based on a particle density of 2.65 g cm⁻³ for the sand and 1.39 g cm⁻³ for the natural soil, divided by the total bulk volume of 173 cm³.

The K_d values for the reference soil exhibited no significant differences between DOC and non-DOC columns ($p > 0.05$); however, substantial variations were observed in CAC-treated soils. Fig. 3 presents a comparison of K_d values on logarithmic scale between CAC-treated soil under standard conditions and after interaction with DOC. The K_d values for CAC-treated soil columns ranged from 8.14 (PFBA) to 7880 L kg⁻¹ (FOSA). The presence of DOC in the system consistently reduced K_d values for all PFASs, confirming that DOC suppresses sorption to CAC. On average, K_d values in the DOC-spiked columns were 0.94 ± 0.34 log units lower ($p = 0.00005$). The strongest impact of DOC was observed for 6:2 FTSA, with a substantial 1.6 orders of magnitude decrease in sorption, followed by FOSA at 1.4 and PFNA at 1.3 orders of magnitude. These findings align with previous studies on PFAS sorption to biochar (Ulrich et al., 2015), suggesting that DOC-mediated sorption reduction is a common phenomenon among carbonaceous sorbents.

K_d values exhibited an increasing trend with increasing perfluoro-carbon chain length for PFCAs and PFASs, indicating a strong positive correlation between the number of carbons and sorption strength. This relationship was highly linear ($R^2 > 0.99$, $p = 0.0004$) for PFCAs with up to eight perfluorocarbons (i.e., PFNA). Additionally, sorption strength was consistently higher for PFASs than PFCAs by ~ 0.15 log units, except for PFNA exhibiting stronger sorption than PFOS. FOSA displayed the highest sorption affinity, with K_d values 1.6 log units greater than PFNA and PFOS, despite having the same perfluoroalkyl chain length. These observations align well with previous studies on PFAS sorption to CAC (Niarchos et al., 2023b, 2022; Sorengard et al., 2019). For 6:2 FTSA, the K_d values appeared higher than PFHxS and PFHpA, however this was not the case when DOC was in solution.

The influence of DOC was stronger for long-chain PFASs compared to their short-chain homologues. This was particularly evident for FTSA and FOSA, with an up to $10^{1.6} = 40$ times decrease in sorption observed in K_d values. This finding is critical, as FTSA and FOSA constitute PFAS precursors, capable of degrading into more stable PFASs (Wang et al., 2013). While these results suggest that DOC can substantially enhance PFAS precursor leachability, it is important to note that our experiments were conducted using a low-organic-carbon subsoil (~ 0.01 % OC). In organic-rich topsoils and sediments, the presence of soil organic matter may provide additional sorption capacity, potentially moderating the DOC effect. Therefore, further studies are needed to assess how DOC influences PFAS mobility across a range of soil types and organic carbon levels, particularly in systems with higher native organic matter content.

3.4. PFAS mass balance and DOC retention

The eluted mass was determined by calculating the AUC of each PFAS breakthrough curve, using the trapezoidal rule, which estimates

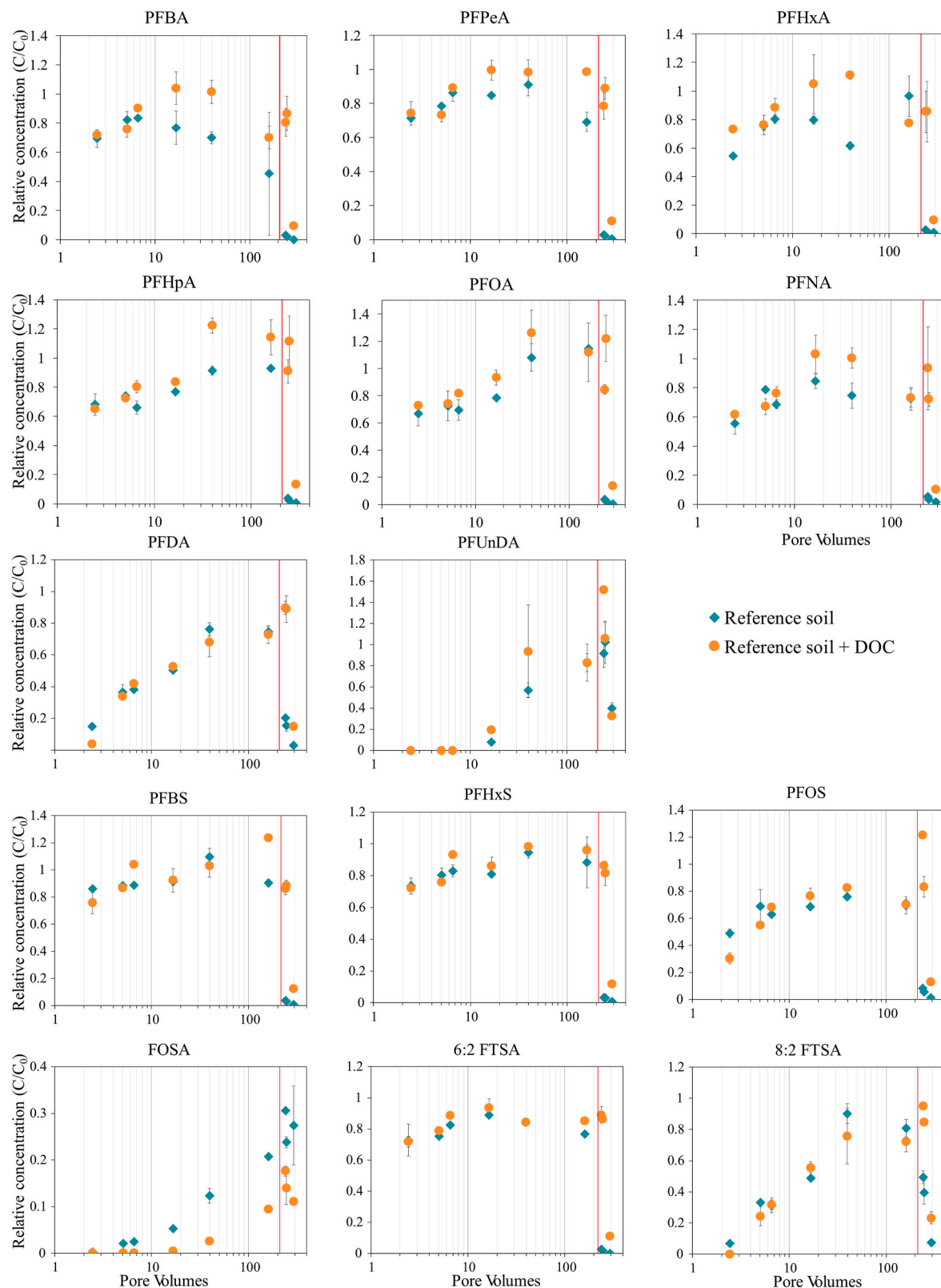


Fig. 1. PFAS breakthrough curves in reference soil and reference soil with DOC-spiked groundwater. The points represent the average C/C_0 of duplicate samples and the error bars their standard deviation. The red line represents the time when spiking stopped, and the inlet solution switched to PFAS-free artificial groundwater (desorption phase). (For interpretation of the references to colour in this figure legend, the reader is referred to the Web version of this article.)

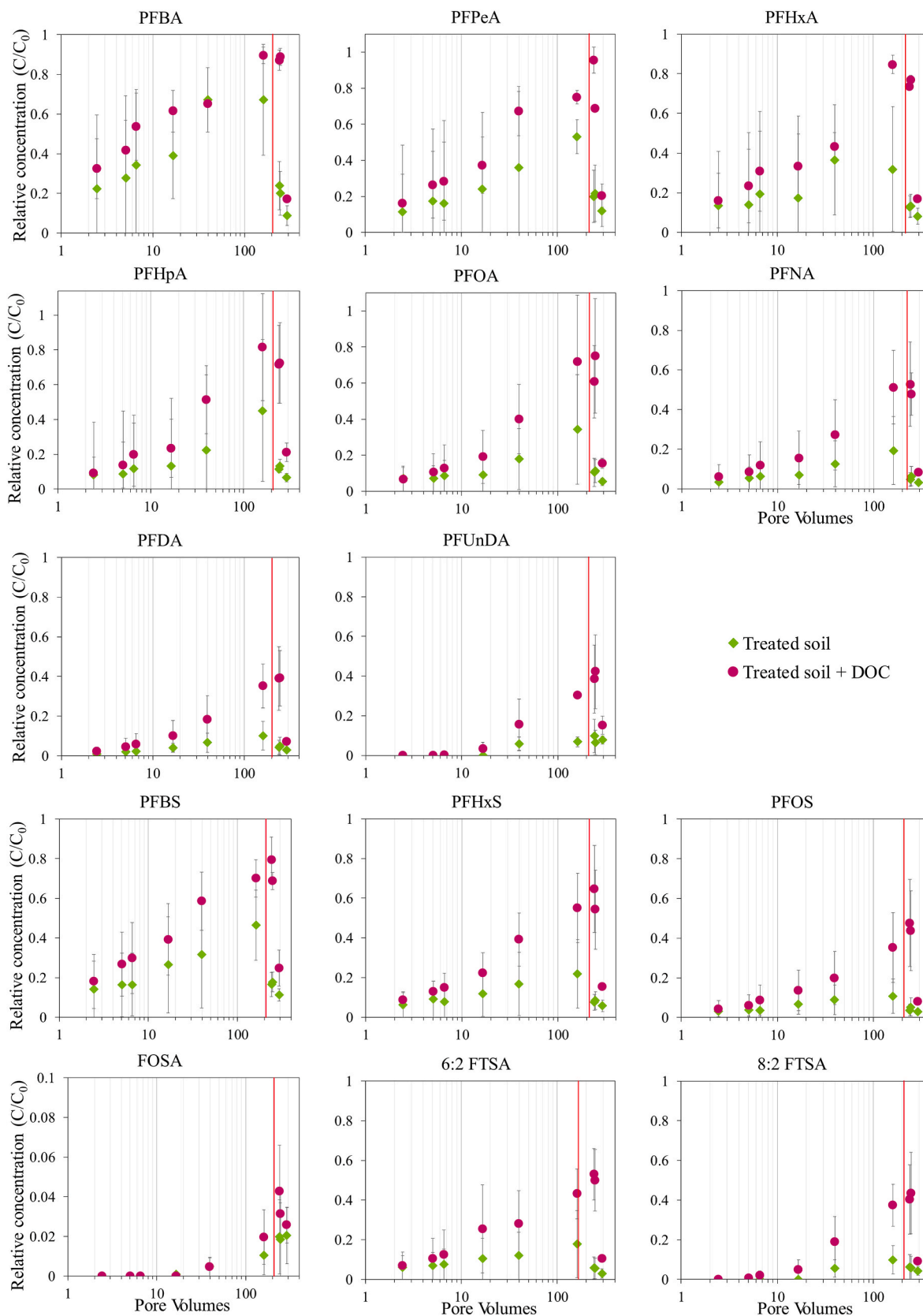


Fig. 2. PFAS breakthrough curves for CAC-treated soil and CAC-treated soil with DOC-spiked groundwater. The points represent the average C/C_0 of duplicate samples and the error bars their standard deviation. The red line represents the time when spiking stopped, and the inlet solution switched to PFAS-free artificial groundwater (desorption phase). Note: for FOSA the y-axis is up to 0.1, instead of 1. (For interpretation of the references to colour in this figure legend, the reader is referred to the Web version of this article.)

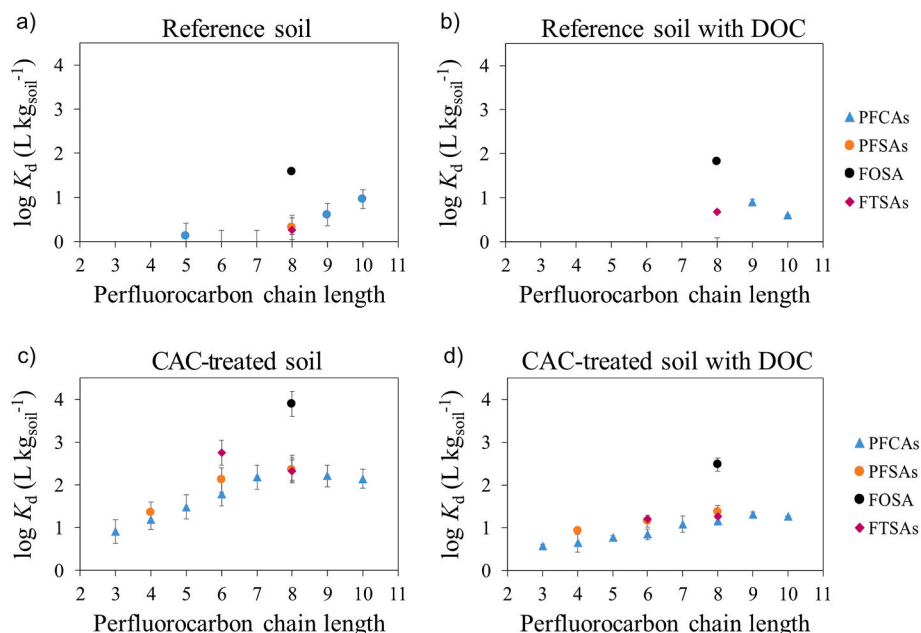


Fig. 3. Soil-water partitioning coefficients (K_d values), for reference (a, b) and CAC-treated (c, d) soil, with and without DOC-spiked groundwater.

the AUC by summing the areas of adjacent trapezoids formed between data points (Table S8 in the SI). The AUC was then multiplied by the measured inlet concentration ($ng\ mL^{-1}$) and the pore volume size (35.05 mL) to obtain the total eluted mass and allow for direct comparison with the injected mass to evaluate PFAS retention or mobilization under different DOC conditions.

The influence of DOC on PFAS retention is further illustrated in Fig. 4, which shows the percentage of eluted mass for each compound across both soil types. DOC addition substantially increased PFAS elution, particularly in CAC-treated soils, supporting the calculated mass

balances (Table S8 in the SI) and emphasizing DOC's role in modulating PFAS mobility. In the absence of DOC, PFAS retention in treated soils was substantial, with eluted mass ranging from just 1–64 % depending on the compound. Long-chain PFASs (e.g., PFOS, PFUnDA, FOSA) exhibited the strongest retention, with only 8–10 % eluted, and FOSA nearly completely retained (1 % eluted). These results demonstrate that CAC can retain a significant amount of especially long-chain PFAS either by very slow desorption kinetics, desorption that only occurs by replacement/competition or partly irreversible sorption characteristics. PFAS sorption-desorption to CAC is complex and the long-term retention

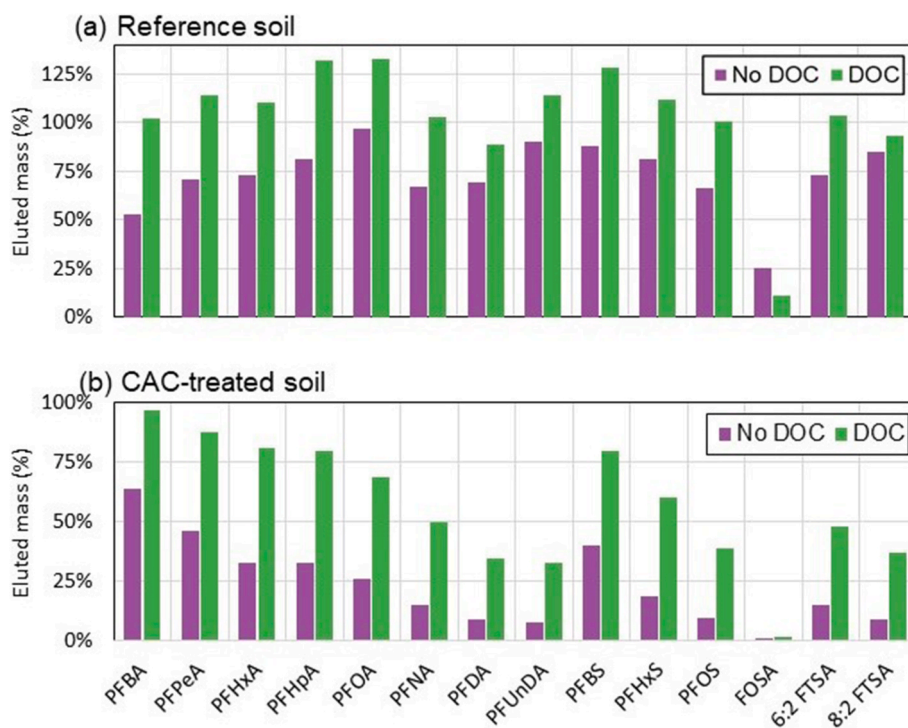


Fig. 4. Eluted mass (%) of PFAS compounds from (a) reference soil and (b) CAC-treated soil columns, under conditions with and without dissolved organic carbon (DOC).

cannot be predicted by equilibrium sorption models. Similar formation of non-extractable PFAS residues (irreversible sorption characteristics) has been observed by e.g. [Zhu et al. \(2021\)](#).

However, when DOC was present in treated soils (T DOC), elution increased across all PFASs, more than doubling for several compounds. For instance, PFHxA elution rose from 33 % to 81 %, PFNA from 15 % to 50 %, and PFOS from 10 % to 39 %. This clearly demonstrates that DOC increases PFAS desorption and reduces PFAS retention in the soil, likely by competing for sorption sites on CAC or forming soluble complexes with PFAS, thereby enhancing mobility.

Similar trends were observed in the reference soil columns. Without DOC, elution ranged from 25–97 %, while with DOC (R DOC), elution exceeded 100 % for many compounds, notably PFHpA, PFOA, PFBS, and PFBS. This suggests that DOC not only enhanced PFAS desorption but also mobilized background PFAS that were previously retained in the soil, or caused minor overestimation due to analytical variability. PFUnDA and PFNA also showed a notable increase (from 90 % to 114 %, and 67 % to 103 %, respectively), further supporting DOC's role in mobilizing even strongly sorbing long-chain PFAS.

These trends align with the post-experimental DOC retention data ([Table S7 and SI](#)), which showed measurable increases in organic carbon content in both reference and CAC-treated columns. In reference soil, there was a 0.01 % uptick in organic carbon content when DOC was present (columns R_{DOC1}, R_{DOC2}), and CAC-treated soil exhibited a greater increase of 0.02 %. This supports the hypothesis that DOC can adsorb to CAC surfaces, possibly altering the sorption environment and contributing to reduced PFAS binding.

4. Environmental implications and conclusions

The study demonstrated that DOC significantly reduces the sorption and increases the desorption of certain PFASs, as evidenced by accelerated breakthrough in both untreated and CAC-treated soils, more markedly in the latter. The observed reduction in sorption capacity suggests competitive interactions between DOC and PFASs for sorption sites, potentially lessening the efficacy of CAC as a stabilization agent in matrices with elevated DOC.

The impact of DOC was particularly strong in CAC-treated soils, where K_d values exhibited substantial reductions, with up to a 40-fold decrease for 6:2 FTSA. The preferential desorption of long-chain PFASs is especially concerning, as these compounds are typically the main targets of stabilization-based remediation. Mass balance calculations further support this finding, showing that PFAS elution in CAC-treated soils increased from as low as 1–10 % to as much as 80–97 % when DOC was present, confirming the strong influence of DOC on reducing retention, even in highly sorptive media.

Overall, these findings are highly relevant for risk assessments of PFAS transport in both treated and untreated soils, reinforcing the necessity of incorporating DOC dynamics into remediation planning. Given that the DOC concentrations employed in this study represent the upper bound of environmentally relevant levels, the findings provide a conservative estimate of worst-case remediation scenarios. Considering the seasonal variability in DOC fluxes, as a response to hydrological events, future investigations should prioritize quantifying the effects of transient DOC levels on PFAS mobilization and long-term remediation stability. Investigations with different hydraulic conductivities can also provide further insights into the influence of retention time on sorption equilibria.

While this study did not include direct measurement of DOC transport, the observed differences between DOC-amended and non-amended columns provide a robust proxy for assessing DOC's influence on PFAS mobility. Future work should incorporate DOC breakthrough curves and molecular-level characterisation, to deepen our understanding of DOC dynamics and interactions. Recent work by [Chen et al. \(2025\)](#) shows that DOM composition, particularly aromaticity and unsaturation, plays a critical role in PFAS mobility, especially for sulfonated compounds.

Incorporating such insights would enhance our understanding of how DOC quality, not just quantity, shapes PFAS behaviour in soil systems.

In summary, our findings suggest that elevated DOC levels can substantially compromise the performance of CAC-based PFAS remediation. Site-specific DOC levels and variability should therefore be carefully considered when planning or evaluating stabilization strategies for PFAS-contaminated soils and groundwater.

CRediT authorship contribution statement

Georgios Niarchos: Writing – review & editing, Writing – original draft, Visualization, Validation, Supervision, Software, Project administration, Methodology, Investigation, Formal analysis, Data curation, Conceptualization. **Lutz Ahrens:** Writing – review & editing, Supervision, Resources, Methodology. **Dan B. Kleja:** Writing – review & editing, Supervision, Methodology. **Anna Merle Liebenehm Axmann:** Methodology. **Fritjof Fagerlund:** Writing – review & editing, Supervision, Methodology, Funding acquisition, Data curation, Conceptualization.

Declaration of competing interest

The authors declare that they have no known competing financial interests or personal relationships that could have appeared to influence the work reported in this paper.

Acknowledgements

This work was financially supported by TUFFO – a research and innovation program on contaminated sites managed by the Swedish Geotechnical Institute (SGI) through the StopPFAS project (1.1-1708-0501).

Appendix A. Supplementary data

Supplementary data to this article can be found online at <https://doi.org/10.1016/j.envpol.2025.126928>.

Data availability

Data will be made available on request.

References

- Ahrens, L., Felizeter, S., Sturm, R., Xie, Z., Ebinghaus, R., 2009. Polyfluorinated compounds in waste water treatment plant effluents and surface waters along the River Elbe, Germany. *Mar. Pollut. Bull.* 58, 1326–1333. <https://doi.org/10.1016/j.marpolbul.2009.04.028>.
- Ateia, M., Maroli, A., Tharayil, N., Karanfil, T., 2019. The overlooked short- and ultrashort-chain poly- and perfluorinated substances: a review. *Chemosphere* 220, 866–882. <https://doi.org/10.1016/j.chemosphere.2018.12.186>.
- Buck, R.C., Franklin, J., Berger, U., Conder, J.M., Cousins, I.T., de Voogt, P., Jensen, A.A., Kannan, K., Mabury, S.A., van Leeuwen, S.P.J., 2011. Perfluoroalkyl and polyfluoroalkyl substances in the environment: terminology, classification, and origins. *Integr. Environ. Assess. Manag.* 7, 513–541. <https://doi.org/10.1002/ieam.258>.
- Carey, G.R., Hakimabadi, S.G., Singh, Mantake, McGregor, R., Woodfield, C., Paul, J., Van Geel, J., Anh, J., Pham, L.-T., 2022. Longevity of colloidal activated carbon for in situ PFAS remediation at AFFF-contaminated airport sites. *Remediat. J.* <https://doi.org/10.1002/REM.21741>.
- Chen, Y., Cao, D., Li, X., Jia, X., Shi, Y., Cai, Y., 2025. Interactive effects of soil dissolved organic matter (DOM) and Per- and polyfluoroalkyl substances on contaminated soil site: DOM molecular-level perspective. *J. Hazard. Mater.* 488, 137372. <https://doi.org/10.1016/j.jhazmat.2025.137372>.
- Dickman, R.A., Aga, D.S., 2022. A review of recent studies on toxicity, sequestration, and degradation of per- and polyfluoroalkyl substances (PFAS). *J. Hazard. Mater.* 436, 129120. <https://doi.org/10.1016/j.jhazmat.2022.129120>.
- Du, Z., Deng, S., Bei, Y., Huang, Q., Wang, B., Huang, J., Yu, G., 2014. Adsorption behavior and mechanism of perfluorinated compounds on various adsorbents-A review. *J. Hazard. Mater.* 274, 443–454. <https://doi.org/10.1016/j.jhazmat.2014.04.038>.
- Fetter, C.W., 2018. *Applied Hydrogeology*. Waveland Press.

- Hansen, M.C., Børresen, M.H., Schlabach, M., Cornelissen, G., 2010. Sorption of perfluorinated compounds from contaminated water to activated carbon. *J. Soils Sediments* 10, 179–185. <https://doi.org/10.1007/S11368-009-0172-Z/TABLES/4>.
- Iubel, J.P.G., Braga, S.M., Braga, M.C.B., 2021. The importance of organic carbon as a coadjutant in the transport of pollutants. *Water Sci. Technol.* 84, 1557–1565. <https://doi.org/10.2166/WST.2021.351>.
- Jeon, J., Kannan, K., Lim, B.J., An, K.G., Kim, S.D., 2011. Effects of salinity and organic matter on the partitioning of perfluoroalkyl acid (PFAs) to clay particles. *J. Environ. Monit.* 13, 1803. <https://doi.org/10.1039/c0em00791a>.
- Johnson, G.R., Brusseau, M.L., Carroll, K.C., Tick, G.R., Duncan, C.M., 2022. Global distributions, source-type dependencies, and concentration ranges of per- and polyfluoroalkyl substances in groundwater. *Sci. Total Environ.* 841, 156602. <https://doi.org/10.1016/j.scitotenv.2022.156602>.
- Kabiri, S., Tavakkoli, E., Navarro, D.A., Degryse, F., Grimison, C., Higgins, C.P., Mueller, J.F., Kookana, R.S., McLaughlin, M.J., 2024. The complex effect of dissolved organic carbon on desorption of per- and poly-fluoroalkyl substances from soil under alkaline conditions. *Environ. Pollut.* 356, 124234. <https://doi.org/10.1016/j.envpol.2024.124234>.
- Kho, C.L.L., Sipler, R.E., Fudge, A.R., Beheshti Foroutani, M., Boyd, S.G., Ziegler, S.E., 2022. Salt-induced flocculation of dissolved organic matter and iron is controlled by their concentration and ratio in boreal coastal systems. *J. Geophys. Res. Biogeosciences* 127, e2022JG006844. <https://doi.org/10.1029/2022JG006844>.
- Klucáková, M., 2018. Size and charge evaluation of standard humic and fulvic acids as crucial factors to determine their environmental behavior and impact. *Front. Chem.* 6, 352896. <https://doi.org/10.3389/fchem.2018.00235/BIBTEX>.
- Li, F., Duan, J., Tian, S., Ji, H., Zhu, Y., Wei, Z., Zhao, D., 2020. Short-chain per- and polyfluoroalkyl substances in aquatic systems: occurrence, impacts and treatment. *Chem. Eng. J.* 380, 122506. <https://doi.org/10.1016/j.cej.2019.122506>.
- Liu, W.X., He, W., Wu, J.Y., Wu, W.J., Xu, F.L., 2019. Effects of fluorescent dissolved organic matters (FDOMs) on perfluoroalkyl acids (PFAAs) in lake and river water. *Sci. Total Environ.* 666, 598–607. <https://doi.org/10.1016/j.scitotenv.2019.02.219>.
- Lønborg, C., Carreira, C., Abril, G., Agustí, S., Amaral, V., Andersson, A., Aristegui, J., Bhadury, P., Bif, M.B., Borges, A.V., Bouillon, S., Calleja, M.L., Cotovicz, L.C., Cozzi, S., Doval, M., Duarte, C.M., Eyre, B., Fichot, C.G., García-Martín, E.E., Garzon-García, A., Giani, M., Gonçalves-Araújo, R., Gruber, R., Hansell, D.A., Hashihama, F., He, D., Holding, J.M., Hunter, W.R., Ibáñez, J.S.P., Ibello, V., Jiang, S., Kim, G., Klun, K., Kowalczyk, P., Kubo, A., Lee, C.W., Lopes, C.B., Maggioni, F., Magni, P., Marrase, C., Martin, P., McCallister, S.L., McCallum, R., Medeiros, P.M., Morán, X.A.G., Muller-Karger, F.E., Myers-Pigg, A., Norli, M., Oakes, J.M., Osterholz, H., Park, H., Lund Paulsen, M., Rosentreter, J.A., Ross, J.D., Rueda-Roa, D., Santinelli, C., Shen, Y., Teira, E., Tinta, T., Uher, G., Wakita, M., Ward, N., Watanabe, K., Xin, Y., Yamashita, Y., Yang, L., Yeo, J., Yuan, H., Zheng, Q., Álvarez-Salgado, X.A., 2024. A global database of dissolved organic matter (DOM) concentration measurements in coastal waters (CoastDOM v1). *Earth Syst. Sci. Data* 16, 1107–1119. <https://doi.org/10.5194/ESSD-16-1107-2024>.
- McClellan, P., Englund, S., Östlund, A., Lindegren, K., Wiberg, K., Ahrens, L., 2017. Removal efficiency of multiple poly- and perfluoroalkyl substances (PFASs) in drinking water using granular activated carbon (GAC) and anion exchange (AE) column tests. *Water Res.* 120, 77–87. <https://doi.org/10.1016/j.watres.2017.04.057>.
- McDonough, L.K., Santos, I.R., Andersen, M.S., O'Carroll, D.M., Rutledge, H., Meredith, K., Oudone, P., Bridgeman, J., Gooddy, D.C., Sorensen, J.P.R., Lapworth, D.J., MacDonald, A.M., Ward, J., Baker, A., 2020. Changes in global groundwater organic carbon driven by climate change and urbanization. *Nat. Commun.* 11, 1279. <https://doi.org/10.1038/s41467-020-14946-1>.
- McDowell, W.H., 2003. Dissolved organic matter in soils—future directions and unanswered questions. *Geoderma* 113, 179–186. [https://doi.org/10.1016/S0016-7061\(02\)00360-9](https://doi.org/10.1016/S0016-7061(02)00360-9).
- Niarchos, G., Ahrens, L., Kleja, D.B., Fagerlund, F., 2022. Per- and polyfluoroalkyl substance (PFAS) retention by colloidal activated carbon (CAC) using dynamic column experiments. *Environ. Pollut.* 308, 119667. <https://doi.org/10.1016/j.envpol.2022.119667>.
- Niarchos, G., Ahrens, L., Kleja, D.B., Leonard, G., Forde, J., Bergman, J., Ribeli, E., Schütz, M., Fagerlund, F., 2023a. In-situ application of colloidal activated carbon for PFAS-contaminated soil and groundwater: a Swedish case study. *Remediat. J.* 33, 101–110. <https://doi.org/10.1002/REM.21746>.
- Niarchos, G., Georgii, L., Ahrens, L., Kleja, D.B., Fagerlund, F., 2023b. A systematic study of the competitive sorption of per- and polyfluoroalkyl substances (PFAS) on colloidal activated carbon. *Ecotoxicol. Environ. Saf.* 264, 115408. <https://doi.org/10.1016/j.ecoenv.2023.115408>.
- Park, M., Wu, S., Lopez, J.J., Chang, J.Y., Karanfil, T., Snyder, S.A., 2020. Adsorption of perfluoroalkyl substances (PFAS) in groundwater by granular activated carbons: roles of hydrophobicity of PFAS and carbon characteristics. *Water Res.* 170, 115364. <https://doi.org/10.1016/j.watres.2019.115364>.
- Penland, T.N., Cope, W.G., Kwak, T.J., Strynar, M.J., Grieshaber, C.A., Heise, R.J., Sessions, F.W., 2020. Trophodynamics of per- and Polyfluoroalkyl substances in the food web of a large Atlantic slope River. *Environ. Sci. Technol.* 54, 6800–6811. https://doi.org/10.1021/ACS.EST.9B05007/ASSET/IMAGES/LARGE/ES9B05007_0005.JPEG.
- Piccolo, A., 2002. The supramolecular structure of humic substances: a novel understanding of humus chemistry and implications in soil science. *Adv. Agron.* 75, 57–134.
- Qi, Y., Cao, H., Pan, W., Wang, C., Liang, Y., 2022. The role of dissolved organic matter during Per- and polyfluorinated substance (PFAS) adsorption, degradation, and plant uptake: a review. *J. Hazard. Mater.* 436, 129139. <https://doi.org/10.1016/j.jhazmat.2022.129139>.
- Ross, I., McDonough, J., Miles, J., Storch, P., Thelakkat Kochunaryanan, P., Kalve, E., Hurst, J., Dasgupta, S.S., Burdick, J., 2018. A review of emerging technologies for remediation of PFASs. *Remediat. J.* 28, 101–126. <https://doi.org/10.1002/rem.21553>.
- Schwarzenbach, R.P., Gschwend, P.M., Imboden, D.M., 2002. *Environmental Organic Chemistry*.
- Schwichtenberg, T., Bogdan, D., Carignan, C.C., Reardon, P., Rewerts, J., Wanzek, T., Field, J.A., 2020. PFAS and dissolved organic carbon enrichment in surface water foams on a Northern U.S. freshwater Lake. *Environ. Sci. Technol.* 54, 14455–14464. https://doi.org/10.1021/ACS.EST.0C05697/ASSET/IMAGES/LARGE/ES0C05697_0005.JPEG.
- Sörensgård, M., Gago-Ferrero, P., Kleja, D.B., Ahrens, L., 2021. Laboratory-scale and pilot-scale stabilization and solidification (S/S) remediation of soil contaminated with per- and polyfluoroalkyl substances (PFASs). *J. Hazard. Mater.* 402, 123453. <https://doi.org/10.1016/j.jhazmat.2020.123453>.
- Sörensgård, M., Kleja, D.B., Ahrens, L., 2019. Stabilization of per- and polyfluoroalkyl substances (PFASs) with colloidal activated carbon (PlumeStop®) as a function of soil clay and organic matter content. *J. Environ. Manage.* 249, 109345. <https://doi.org/10.1016/j.jenvman.2019.109345>.
- Sörensgård, M., Kleja, D.B., Ahrens, L., 2019. Stabilization and solidification remediation of soil contaminated with poly- and perfluoroalkyl substances (PFASs). *J. Hazard. Mater.* 367, 639–646. <https://doi.org/10.1016/j.jhazmat.2019.01.005>.
- Totsche, K.U., Danzer, J., Kögel-Knabner, L., 1997. Dissolved organic matter-enhanced retention of polycyclic aromatic hydrocarbons in soil miscible displacement experiments. *J. Environ. Qual.* 26, 1090–1100. <https://doi.org/10.2134/jeq1997.00472425002600040021X>.
- Ulrich, B.A., Im, E.A., Werner, D., Higgins, C.P., 2015. Biochar and activated carbon for enhanced trace organic contaminant retention in stormwater infiltration systems. *Environ. Sci. Technol.* 49, 6222–6230. https://doi.org/10.1021/ACS.EST.5B00376/SUPPL_FILE/ES5B00376_SI_001.PDF.
- United Nations Environment Programme (UNEP), 2009. Report of the Conference of the Parties of the Stockholm Convention on Persistent Organic Pollutants on the Work of its Fourth Meeting.
- USEPA, 2022. PFAS[EPA: PFAS structures in DSSTox (update August 2022) [WWW Document]]. URL: <https://comptox.epa.gov/dashboard/chemical-lists/PFA-SSTRUCTV5> (accessed 7.17.24).
- USEPA, 1999. Understanding variation in partition coefficient, K_d, values volume I: the K_d model. *Methods of Measurement and Application of Chemical Reaction Codes*.
- Van Glubb, S., Brusseau, M.L., Yan, N., Huang, D., Khan, N., Carroll, K.C., 2021. Column versus batch methods for measuring PFOS and PFOA sorption to geomed. *Environ. Pollut.* 268, 115917. <https://doi.org/10.1016/j.envpol.2020.115917>.
- Vidon, P., Hill, A.R., 2004. Denitrification and patterns of electron donors and acceptors in eight riparian zones with contrasting hydrogeology. *Biogeochemistry* 71, 259–283. <https://doi.org/10.1007/S10533-004-9684-1>.
- Voisin, J., Cournoyer, B., Marjolet, L., Vienney, A., Mermillod-Blondin, F., 2020. Ecological assessment of groundwater ecosystems disturbed by recharge systems using organic matter quality, biofilm characteristics, and bacterial diversity. *Environ. Sci. Pollut. Res.* 27, 3295–3308. <https://doi.org/10.1007/S11356-019-06971-5/FIGURES/5>.
- Wang, Yu, Chang, W., Wang, L., Zhang, Yinfeng, Zhang, Yuan, Wang, M., Wang, Yin, Li, P., 2019. A review of sources, multimedia distribution and health risks of novel fluorinated alternatives. *Ecotoxicol. Environ. Saf.* 182, 109402. <https://doi.org/10.1016/j.ecoenv.2019.109402>.
- Wang, Z., Cousins, I.T., Scheringer, M., Hungerbühler, K., 2013. Fluorinated alternatives to long-chain perfluoroalkyl carboxylic acids (PFCAs), perfluoroalkane sulfonic acids (PFASs) and their potential precursors. *Environ. Int.* 60, 242–248. <https://doi.org/10.1016/j.envint.2013.08.021>.
- Wen, W., Xia, X., Chen, X., Wang, H., Zhu, B., Li, H., Li, Y., 2016. Bioconcentration of perfluoroalkyl substances by Chironomus plumosus larvae in water with different types of dissolved organic matters. *Environ. Pollut.* 213, 299–307. <https://doi.org/10.1016/j.envpol.2016.02.018>.
- Werner, B.J., Lechtenfeld, O.J., Musolf, A., De Rooij, G.H., Yang, J., Gründling, R., Werban, U., Fleckenstein, J.H., 2021. Small-scale topography explains patterns and dynamics of dissolved organic carbon exports from the riparian zone of a temperate, forested catchment. *Hydrol. Earth Syst. Sci.* 25, 6067–6086. <https://doi.org/10.5194/HESS-25-6067-2021>.
- Woodlief, T., Vance, S., Hu, Q., Dewitt, J., 2021. Immunotoxicity of Per- and polyfluoroalkyl substances: insights into short-chain PFAS exposure. *Toxics* 9, 100. <https://doi.org/10.3390/TOXICS9050100>. Page 100 9.
- Zhu, X., Song, X., Schwarzbauer, J., 2021. First insights into the formation and long-term dynamic behaviors of nonextractable perfluorooctanesulfonate and its alternative 6: 2 chlorinated polyfluorinated ether sulfonate residues in a silty clay soil. *Sci. Total Environ.* 761, 143230. <https://doi.org/10.1016/j.scitotenv.2020.143230>.